Proceedings Paper:
Chauhan, M orcid.org/0000-0001-9742-5352, Mattos, LS, Caldwell, DG et al. (1 more author) (2016) Design and modeling of novel modular 2 DOF microsurgical forceps for transoral laser microsurgeries. In: 2016 IEEE International Conference on Advanced Intelligent Mechatronics (AIM). 2016 IEEE International Conference on Advanced Intelligent Mechatronics (AIM), 12-15 Jul 2016, Banff, AB, Canada. IEEE , pp. 1339-1344. ISBN 978-1-5090-2066-9

https://doi.org/10.1109/aim.2016.7576956

Design and Modelling of Novel modular 2 DOF microsurgical forceps for Trans-oral Laser Microsurgeries

Manish Chauhan, Leonardo S. Mattos, Darwin G. Caldwell and Nikhil Deshpande
Department of Advanced Robotics, Istituto Italiano di Tecnologia (IIT), Via Morego 30, Genova, 16163, Italy
Email: {manish.chauhan, leonardo.mattos, darwin.caldwell, nikhil.deshpande}@iit.it

***Abstract*—Transoral Laser Microsurgeries (TLM) are complex otolaryngological procedures requiring the surgeons to perform intraoperative tissue manipulation with great level of control, accuracy and precision. The process involves the use of a surgical laser to treat abnormalities in the throat without any external incisions. The best removal of the malignant tissue is possible only with coordinated control of the laser aiming for incision and the microsurgical tools for orienting and stretching the tissue. However, the traditional microsurgical tools are long, single purpose, one degree-of-freedom (DOF), rigid tools with small range of motion and a traditional grasping handle inducing non-ergonomic usage. Additionally, there are different variety of microsurgical tools with different modes of actuation for the forceps jaws, i.e. in one mode push action of inner translating rod closes the forceps jaws and in other mode the same action opens the jaws. This paper presents a novel, modular microsurgical tool design to overcome the challenges of the traditional tools and improve the surgeon-tool usage experience. The novel design adds a rotational DOF to expand the reach and functionality of the tool. The device is provided with an ergonomic grasping handle that avoids extreme wrist excursions. A straight line motion mechanism is synthesized such that it is capable of adapting to the variety of tools used in TLM within the same device design. This mechanism was validated by ADAMS simulation as well. The proposed new design adds benefits of functional and ergonomic usage for the surgeons, potentially simplifying the surgical tasks.**

I. Introduction

Otolaryngeal procedure's are performed on the oropharynx which can be considered anatomically as a irregularly shaped cylinder. Oropharyngeal cancers, by definition, lie within this cylinder. In order to access and resect a certain subset of these tumors, this cylinder needs to be opened [1]. Transoral Laser Microsurgeries (TLM) involve treatment of these malignancies without any external incisions by the use of a surgical laser in the upper aero-digestive tract (UADT). TLM is beneficial from perspective of lower morbidity and improved organ preservation [2], [3]. The surgical site is exposed using a laryngoscope which allows a direct line-of-sight for the surgical microscope. A CO_2 laser beam is used to either ablate or remove the abnormality. The beam is aimed at the surgical area (area 40 x 40 mm^2) from a distance of 400 mm. The surgical site in TLM (Fig.1), i.e., the vocal cords varies in size from 17–21 mm (males) to 11–15 mm (females) [4]. Such small structure and size of the vocal cords demand a great level of accuracy and dexterity from the surgeon for proper tissue positioning, manipulation and positioning at sub-mm scale.

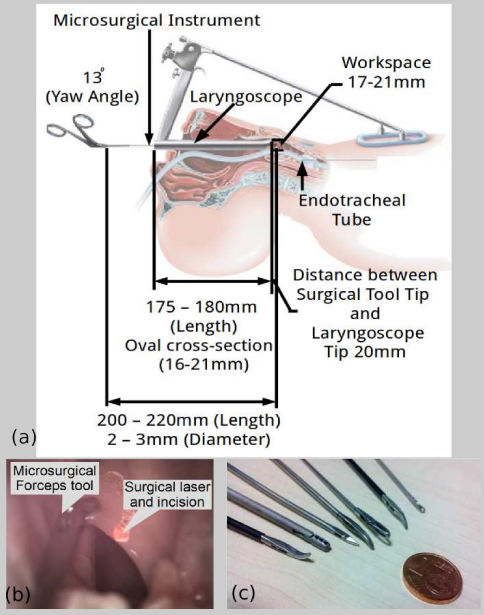

Top - (1a) Cross-sectional view of TLM surgical area. **Bottom Left – (1b)** Microsurgical forceps keeping the vocal cord tissue in traction during laser cutting. **Bottom Right – (1c)** Types of microsurgical tools in TLM.

Figure 1. Traditional setup in TLM operating room

State-of-the-art tools (Fig. 2) used in TLM are pre-curved single purpose, one degree-of-freedom (DOF i.e., open/close of forceps jaws) long and rigid, with a traditional grasping handle at the proximal end, an average shaft length of about 200-220 mm and finally a small yaw angle of 13° [5]. The tools are inserted through the laryngoscope and manually operated for assistive tissue manipulation (like grasping, maneuvering, stretching, removal etc). The best removal of the malignant tissue is possible only with simultaneous coordinated control of the laser aiming for incision and the microsurgical tools for orienting and stretching the tissue perpendicular to the laser path. Achieving these goals is difficult and error-prone: (i) the surgeons are operating long tools with small distal openings in extremely restricted workspaces; (ii) the hand and wrist positions during the procedure are non-ergonomic inducing tremors and wrist excursions over the

long surgical hours; (iii) the surgeons are vulnerable to stress and fatigue in the hands which can directly impact the safety of the operations; and (iv) the coordinated control requires considerable skill during a time-consuming procedure which can be developed only after long hours of extensive training.

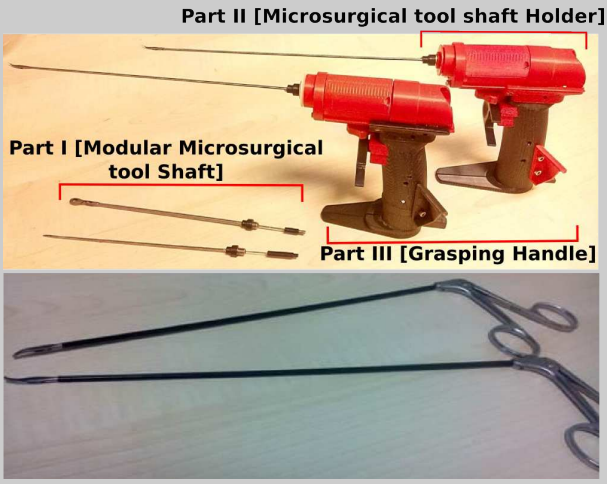

Figure 2. Comparison of new microsurgical forceps (top) with traditional microsurgical forceps (bottom)

The research in this paper addresses the design limitations in the traditional, manual, microsurgical forceps. A new design of the microsurgical forceps is presented for improving tool operation and surgeon interface. The main components of the novel design are: (i) a rotational DOF in addition to the open/close DOF; (ii) a grip-locking mechanism to maintain forceps jaws in closed position; and (iii) an ergonomic handle including a push-button for open/close of the forceps jaws. This handle houses a straight line mechanism for adapting to different types of microsurgical tools. Figure 2 (top) depicts the new design of microsurgical forceps in comparison with traditional forceps (bottom). The novel forceps proposes the following benefits over traditional forceps: (i) allowing the surgeon to grip- n-turn the tissue facilitating better exposure of the site perpendicular to laser beam and enhanced tissue manipulation without operational stress; (ii) facilitating access to different parts of the vocal cords with single tool by using the rotational DOF. Removing the need to use different tools for different parts; (iii) ability to lock the forceps with gripped tissue allowing simpler control of tissue positioning and traction; (iv) ability to use different types of microsurgical tools with the same device design, allowing modularity and (v) easy-to-use, ergonomic and comfortable handling of the tool.

II. Previous Work

In surgical procedures, hand-held surgical tools are under re-examination for their functionality and usability. There are a number of manually operated surgical tools available commercially such as the art2DRIVE [6], art2CURVE [7], and the SILS Hand Instruments [8]. The primary application of these tools are general single port surgical procedures like Laparoscopic, Gynecological, Bariatric, Colorectal, Urological, Cardio-thoracic procedures etc. These commercial tools provide ergonomic grasping handles and allow two-dimensional tool-tip articulation (bending and rotation). They generally have a tool-shaft diameter of about 5 mm and use a remote-center-of-motion (usually the laparoscopic incision port on the patient body) as a pivot point against which the tools can be articulated at the surgical site in nearly hemispherical space. But these tools seldom find their application in microsurgical procedures such as TLM because the principle of operation is based on utilization of pivot point on the body of the patient. In state-of-the-art TLM, the microsurgical tools tend to have a maximum shaft diameter of 3 mm, and the surgeons use the tools in free space without a remote pivot point. These commercial tools are therefore deemed inappropriate for the TLM surgical procedure. Yet, as noted earlier, advanced functionalities in the traditional one-dimensional tools of TLM are highly desirable. The SerpENT articulating instruments [9] are the only commercially available tools that come close to the TLM application area. The tools allow up to 240° bending in one dimension allowing an increased reach for the forceps jaws, while also giving seven different bending-lock positions. The limitations of these instruments: (i) the continued use of the non-ergonomic grasping handles, and (ii) the sub-optimal tool-shaft lengths (~140 mm vs. the desired ~200 mm), constrain their adoption in TLM.

The focus of this research was to redesign the traditional microsurgical tools in TLM from a human-tool interaction perspective in order to stay as close as possible to existing designs as illustrated in Fig. 1 and simultaneously enhance the performance of surgeons. The goal was to create a uniform tool interface for the surgeon with added functionality, i.e., rotational DOF and grip-locking to improve the usability and ergonomics.

III. Design of the Novel Modular Microsurgical Forceps

Considering the constraints offered by TLM surgical setup, the novel design was based on a modular architecture consisting of three components: (i) the modular tool shaft; (ii) the microsurgical tool-shaft holder; and (iii) the grasping handle. (Refer Fig. 2). Both, the microsurgical tool-shaft holder and the grasping handle are fabricated for both right and left handed people using ABS-plastic through additive manufacturing technology, thus making low-cost rapid prototyping a key feature of the design.

A. The modular tool shaft

The tool shaft is a modified version (maintaining the same length of 200∼220 mm) of existing microsurgical tools used in TLM. The traditional forceps (Fig. 3a) are made up of an outer shaft (ϕ 2.5 mm) which holds an inner translating rod (ϕ 1 mm). The translation of this rod (motion of about 3 mm) provides the open-close DOF, where the jaws move from completely open to closed configuration. Two adaptations, namely Uniform Docking Interface 1 and 2 are introduced in the tool shaft (Fig. 3b).

- Uniform Docking Interface 1: Here a short, 3D printed, cylindrical tube is placed to hold an M6 grub screw at the proximal end of tool shaft. This grub screw is customized to be hollow along its central axis.
- Uniform Docking Interface 2: An extension is fixed to the inner transting rod with a M3 srew at its distal end. Actuating this extension by a suitable mechanism provides the open/close DOF of microsurgical tool jaws.

The two interfaces are introduced in different tool shafts, allowing compatibility for tools with different tool-jaw types (as shown in Fig. 1c) with the same device design. This introduces interchangeability and modularity in the device.

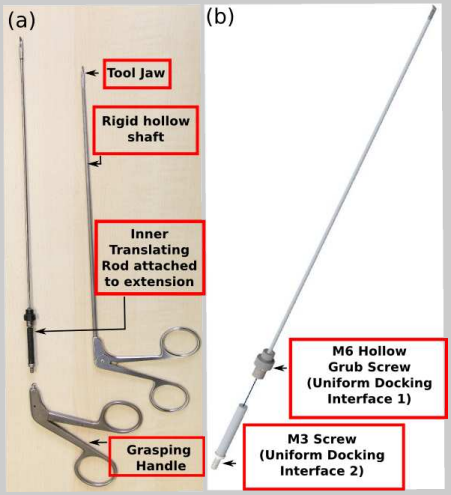

Left - (3a) Dis-assembled traditional forceps **Right** - (3b) Modifications introduced in tool shaft

Figure 3. Modification to existing microsurgical tools

B. The microsurgical tool-shaft holder

This component forms the backbone of the design and incorporates the mechanisms for the open/close and rotational DOFs.

- The rotational DOF is introduced with the help of an anti-backlash miter gear assembly (Nordex LHS E2-30). The inner translating rod extension of the modular tool shaft (Fig.4) passes through the axial miter gear and attaches to a deep groove ball bearing (SKF 618/7) fixed inside a frictionless slider assembly. This decouples the rotation of microsurgical tool from its open/close DOF. The outer shaft of tool docks into the *axial* miter gear through the M6 screw joint (Uniform Docking Interface 1). A rotation knob is coupled to the *normal* miter gear through a set of spur gears allowing manual rotation of the modular tool. The design of the rotation knob and its location was finalized through a consultative process with different users for improving the ergonomics of the device. The rotation knob is controlled by either the thumb or the index finger, providing 360° rotation of the tool shaft in both clockwise and anti-clockwise direction.
- A friction-less slider assembly actuated by a six link mechanism capable of generating straight line motion (housed in the grasping handle) is attached to the inner translating rod (Uniform Docking Interface 2). This provides the open/close of the forceps jaws. The synthesis of the mechanism is described in Section IV.

The design of the mechanism allows simultaneous control of the rotation and open/close of the forceps jaws.

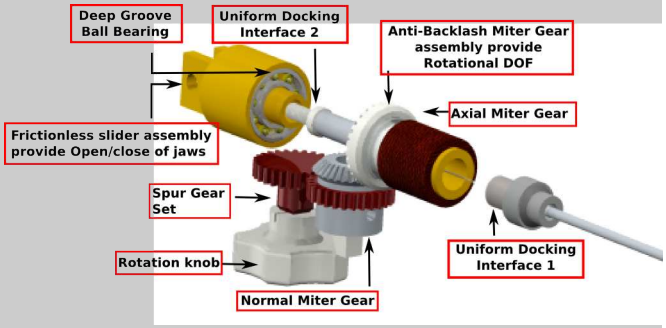

Figure 4. Perspective view of the design showing the two DOFs and the uniform docking system.

C. The grasping handle

The traditional microsurgical forceps have a traditional scissor-like grasping handle (Fig. 2) which induces non ergonomic hand and wrist positions during the procedure inducing tremors and wrist excursions over the long surgical hours. Bending the wrist whilst performing the surgery that requires repeated rotation or twisting of the forearm, can also induce repeated stress at the elbow joint causing irritation and swelling. In order to avoid stress and maintain neutral wrist positions, cylindrical grasping handle is considered optimal [10], [11] for improved application of force on tissue. (i) The cylindrical grip diameter and height of the handle was considered optimal to be between 60∼90 mm and 70∼140 mm range respectively [12], such that it could be useful for both male and female. (ii) The actuation of the device was preferred to be done by the index finger in order to have maximum force application on tissue. (iii) The length of the complete device is considered optimal to be within 300 mm in order to be operational comfortably within the 400 mm range as discussed in I. Maintaining this as the basic principle, the design of the handle was based on ergonomic principles to avoid wrist excursions during tissue manipulation and was inspired from the design of computer graphics and gaming joysticks [13], [10]. Tissue manipulation during TLM demands continuous maintainence of constant force application, hence a stable ergonomic grip is desirable for better device handling.

The assembly of the tool shaft and the tool-shaft holder docks into the grasping handle by sliding through the provided guide-ways. The grasping handle houses an ergonomically designed push-button guided by a compression spring, which serves to open/close the forceps gripper jaws by pressing action. A set of linkages are actuated by the push-button in order to provide the linear translation of the slider assembly through kinematic inversion. This kinematic chain

of linkages are designed for straight line motion generation of the slider assembly, as described in IV.

Figure 5 shows the internal design of the push-button mechanism. It consists of an ergonomically designed button (E_P), which has extension bars on its circumference (E_b). Two versions of this button is designed which has extension bars suitable for both right and left handed surgeons. The button (E_P) fits into link (PB_1) by press fit. A deep groove ball bearing (SKF 618/7) (B_E) connects link (PB_1) with (PB_2), which allows link (PB_1) to rotate about its axis independently with respect to link (PB_2). The link (PB_2) is rigidly connected to yet another in-axis link (S_L) which translates centrally through a compression spring (C_S) (provided between its box casing and link (PB_2)), passes through a hole h provided in the box casing. The displacement of the assembly of these linkages linearly translates the slider assembly (Fig. 4). The compression spring helps the link's to return back to home position.

An additional feature of this design is its ability to lock when the forceps gripping jaws are completely closed. This is possible with the help of extension bars (E_b). As explained in Section III-A, a translation of 3 mm for inner translating rod moves the gripper jaws from completely open to closed configuration. Thus, a T-shaped cavity in the box casing cap is provided such that the protrusion P_t on link (PB_1) translates for 3 mm through this cavity and engages with the wall's of T (on rotation with thumb) in order to lock. Figure 5 shows the top view of the T-shaped cavity and the locking mechanism where the push-button is pressed into gripper close position. Shifting the extension bars (E_b) down with the thumb action locks the grip, while shifting the levers up again releases the lock.

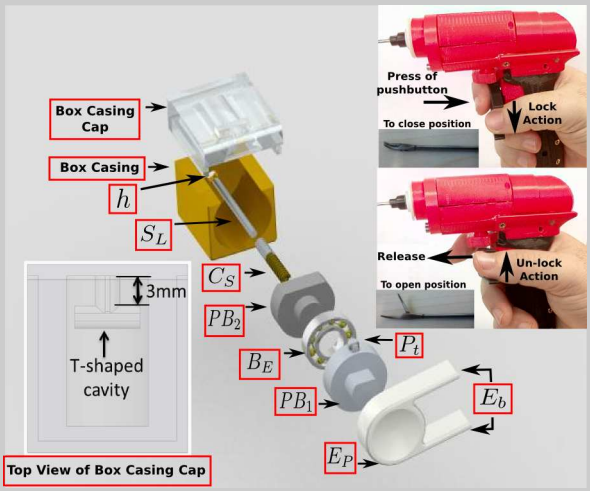

Figure 5. Exploded view of push-button mechanism

IV. Kinematic Synthesis of the Mechanism

The translation mechanism for the open/close DOF is designed as a three-stage problem where a six-link mechanism is synthesized as a Function Generator problem (where output motion is linearly coordinated with input actuation) using the 3 position synthesis graphical method. In the first stage of synthesis, a slider crank mechanism is designed which follows a straight line trajectory along the direction of the slider assembly from fig. 4. In the second stage, the slider crank is converted into a four-bar mechanism. Finally, a six-link mechanism is created in order to satisfy Grubler's criterion [14] for single degree of freedom constant mechanism. Two pairs of coordinated input/output motions are chosen such that the crank rotation angles $\left(\theta_2^{1,2},\theta_2^{2,3}\right)$ correspondingly produce slider displacement $\left(s^{1,2},s^{2,3}\right)$. Here $\left(\theta_2^{1,2},\theta_2^{2,3}\right)$ correspond to rotation of crank from angular position 1 to 2 and 2 to 3 respectively. And corresponding coordinated slider displacement is shown by $\left(s^{1,2},s^{2,3}\right)$.

A. Stage 1

The graphical method of kinematic synthesis of stage 1 mechanism begins with arbitrary choice of hinge point $O_2^{'}$ as shown in Fig. 6. In light of previous discussion, maximum displacement of the slider assembly is 3 mm and in order to generate a straight line along this path, three Chebyshev's precision points were chosen utilizing the equation

$$x_j = a - hcos[(2j-1)\pi/2n]$$

where $a = (x_i + x_f)/2$ and $h = (x_f - x_i)/2$. Here x_i and x_f are the initial and final position of slider motion i.e. 0 and 3 mm correspondingly. Also, n refers to total number of Chebyshev's precision points which is three in this case. And j refers to the each individual precision point i.e. j_1, $j_2$and j_3. Hence the three precision points where the straight line motion must be followed accurately were $x_1 = 0.2$ mm, $x_2 = 1.5$ mm and $x_3 = 2.799$ mm. These precision points are correspondingly indicated in Fig. 6a and 6b as B_1, B_2, B_3. Point O_2 is chosen at an offset (e) of 18 mm and distance (X) of 20 mm from line of sliding action because of space constraints in the designed device. The direction of sliding action is chosen to be positive x direction and crank rotation angle $\left(\theta_2^{1,2},\theta_2^{2,3}\right)$ are chosen to be positive in clockwise direction.

Point A_1 is located by precision point x_1. In order to obtain the crank (O_2A) and the connecting rod length (AB) the principle of kinematic inversion is utilized where the crank rod is held fixed at the first configuration corresponding to the first precision point x_1 such that point B_1 moves in a circle with point A_1 as centre. Thus following the method locates the inverted position of point A_1 corresponding to first configuration B_1 at the same position $A_1^{'}$ and $B_1^{'}$. In order to obtain the inverted position of precision point B_2, the crank point A_1 is rotated by $\left(\theta_2^{1,2}\right)$ in anti-clockwise direction. This inversion locates the new $A_1^{'}$ at $A_2^{'}$. Since the physical link length between point B_2 and $A_1^{'}$ does not change, the same distance locates $B_2^{'}$ as shown in figure 6a and 6b. Similar steps are followed to obtain the inverted position for precision point B_3, but this time the crank rod is rotated by angle $\left(\theta_2^{1,3} = \theta_2^{1,2} + \theta_2^{2,3}\right)$ in anti-clockwise direction to obtain the inverted points $A_3^{'}$ and $B_3^{'}$. Hence

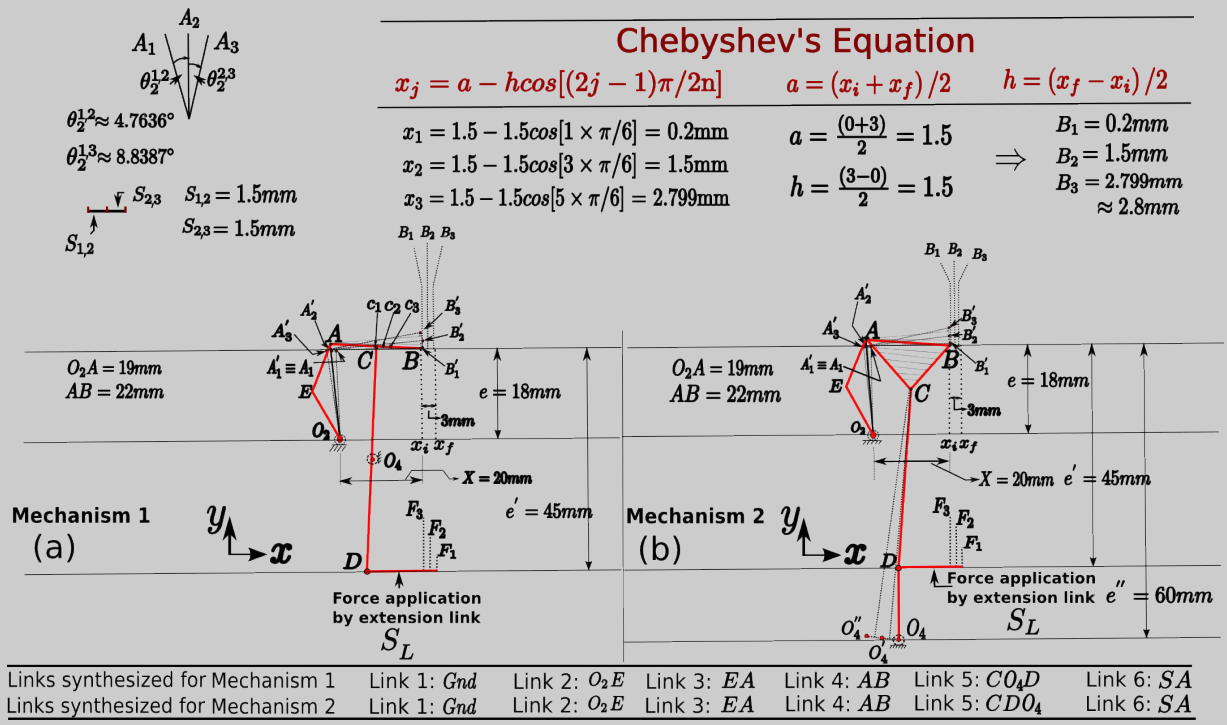

Note: Point B in above figure is representative of the slider assembly (SA); $Gnd \equiv$Ground

Figure 6. Kinematic Synthesis using Function Generation Graphical Method

three set of inverted points are $\left(A_1', B_1'\right)$, $\left(A_2', B_2'\right)$ and $\left(A_3', B_3'\right)$ as seen in Fig.6.

Now, the crank pin point A is obtained by a circle passing through the points B_1', B_2', B_3'. This point is obtained at the point of intersection of the perpendicular bisector's of line connecting (B_1', B_2') and (B_2', B_3'). The required slider crank mechanism $O_2 - A - B$ is thus obtained which is capable of generating a straight line along the three Chebyshev's precision points.

B. Stage 2

The second stage of the mechanism design process was challenging as there exist two different kind of tool shafts: (i) Mechanism 1 - pushing action of inner translating rod closes the tool jaws and; (ii) Mechanism 2 - pushing action open's the tool jaw. In order to make the device universally adaptable to any kind of tool shaft, two different mechanisms were designed by doing small modification to the above designed mechanism $O_2 - A - B$. Special attention was paid to house both the mechanisms in the same device design.

1) Mechanism 1: As is seen in Fig. 6a, coordinated linear relationship mechanism between the ergonomic push-button and slider assembly was maintained such that positions F_1 to F_2 and then to F_3 should move the slider through positions B_1, B_2, B_3 correspondingly. In order to meet the design space constraints (as discussed in III-C) in the physical device, the choice of actuation point of above designed slider crank mechanism was finalized by following principle of kinematic inversion in order to locate the actuation point, D. As the connecting rod (AB) passes through three precision positions, it's mid-point C follow positions C_1, C_2, C_3. These three points lie on a circle, whose centre is located by the intersection of the perpendicular bisectors of the lines joining the points (C_1, C_2) and (C_2, C_3). This intersection point (namely point D) is at an offset e' of 45 mm from the sliding line of action. With introduction of fourth link between the points C and D, the above designed slider crank was converted into four bar mechanism. This link (CD) is actuated at point D by an extension link (S_L) from the push-button assembly in Fig.5. The link (CD) is hinged at it's mid-point O_4 so that on actuation (which is by pushing of push-button through point F_1, F_2 and F_3) at point D, there is a motion inversion for point C and in-turn pushing of the slider assembly (link 6). This unique inversion of motion adapts to the forceps tool where push action of inner translating rod closes the forceps jaws. The design also conformed to ergonomic principles where the user needs to perform intuitive action with a push-button for closing the forceps.

2) Mechanism 2: Principle of kinematic inversion and the coordinated function generation method was again utilized for the design of mechanism shown in Figure 6b. An arbitrary position of hinge point O_4 was chosen at an offset of e'' of 60 mm from the line of sliding action. This point was chosen due to space constraints (III-C) in the physical device. According to the principle of kinematic inversion, the slider crank designed in first stage was held fixed in first configuration position i.e. point B coincides with initial position $x_i = 0$ and point O_4 moves in a circle with A as centre. With reference to previous explaination, two inverted

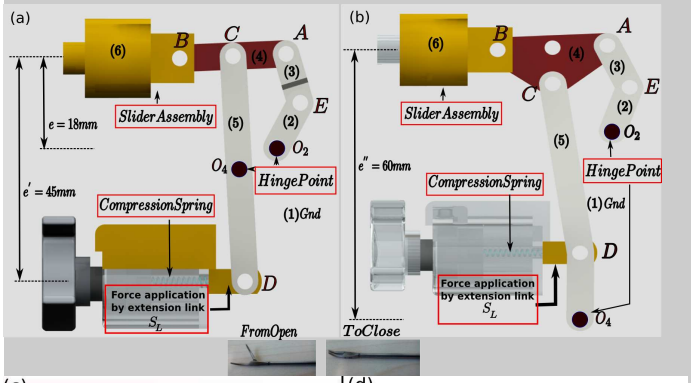

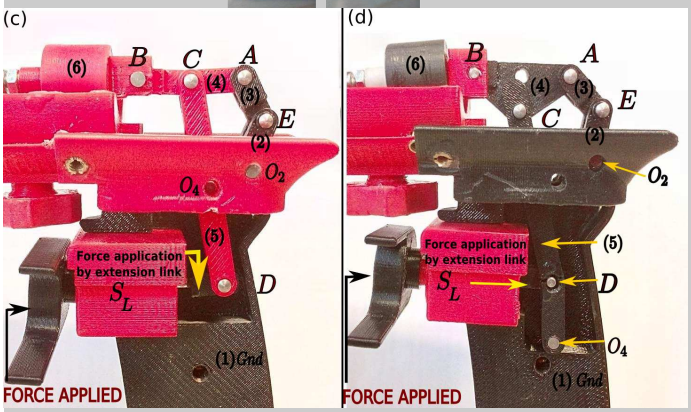

(7a, 7b) Top - CAD model dimensional comparison of two synthesized mechanisms. **(7c, 7d) Bottom -** Real prototype based on both mechanisms

Figure 7. Forceps Jaw Open/close mechanism

position of hinge point O_4were obtained namely $O_4^{'}$ and $O_4^{''}$corresponding to positions A_2-B_2 and A_3-B_3. The three points O_4, $O_4^{'}$ and $O_4^{''}$ lie on a circle whose centre C is found by intersection of perpendicular bisectors on line joining above three points. Finally a triangular shape connecting rod link $A-B-C$ is obtained which is connected to the fourth link $C-D-O_4$ at point C. The location of actuation of the mechanism remains at the same offset distance $e^{'}$and force is applied at point D by extension link (S_L) to actuate slider assembly (link 6). This mechanism adapt's to the forceps tool where push action of inner translating rod opens the forceps jaws.

C. Stage 3

Finally, on performing mobility analysis using the Grübler's criterion (Degree of Freedom$= 3\,(n-1)-2j-h$, where n= Number of links, j= Number of lower pair and h= Number of higher pair) for single DOF constant mechanism, it was found that the DOF of above designed mechanism is zero. This could be explained from the fact that link (ACB) is connected to a sliding bar which does not allow the mechanism to move in vertical y direction. This constraints makes the linkage rigid with no motion. The mechanism can work if there is in-built flexibility in crank link (O_2A). In order to satisfy the Grubler's criterion, an additional link was introduced between points O_2 and A at the point E. This location of point E was arbitrarily chosen at the middle of the offset e in order to meet the design space constraint as enumerated in III-C.

A suitable 6 link single DOF mechanism for the forceps was successfully fabricated based on the graphical method of function generation using Chebyshev's precision points in three stages. Figure 7a, b show the CAD model of the above synthesized mechanism and Figure 7c, d show the final prototype of the device grasping handle encasing the mechanisms in them.

Table I
TOTAL NUMBER OF LINKS SYNTHESIZED AT END OF EACH STAGE

Stage	Number of linkages synthesized	Name of the links
1	4	Gnd, (O_2A), (AB), SA
2	5	Gnd, (O_2A), (AB), SA, (CD)
3	6	Gnd, (O_2E), (EA),(AB), SA, (CO_4D) for Mechanism 1; (CDO_4) for Mechanism 2.

Note: Ground≡Gnd; slider assembly≡SA

V. Validation of Kinematic Model with ADAMS Simulation

An ADAMS simulation modelling was performed to validate the designed mechanisms for generation of straight line motion. The simulation was performed by applying constant linear force (representing force applied through extension link (S_L)) at point D on link (CO_4D) for Mechanism 1 and (CDO_4) for Mechanism 2 . As it can be seen from Fig. 8a and b, the centre of mass of the slider assembly (link 6) follows a straight line motion for the range of motion of 3 mm as per design specifications.

VI. Conclusions and Future Work

Design of a novel, modular microsurgical device to overcome the challenge of traditional tools is presented here which is capable to accomodate any kind of surgical tool shaft by adding a rotation DOF in the tool in addition to tool open/close. The device is provided with an ergonomic grasping handle that avoids extreme wrist excursions. Two straight line mechanisms are synthesized which are housed inside the tool design are presented. The mechanism design is validated with the help of ADAMS simulation. The tool is designed keeping in mind the ergonomic principles of tool usage as it is provided with actuation push-button which is capable of locking the forceps in completely closed position. The new forceps complies with design specifications enumerated in III-C and offers functional and ergonomic benefits over its counterpart.

On preliminary comparitative analysis with the traditional microsurgical forceps, the proposed new forceps tool is bigger in size. The current version of the tool is higher in weight (190∼200gms) with respect to traditional devices (40∼50gms). Hence, design optimization will be performed in future in order to reduce the size and weight of the device while maintaining the additional features. Also, work will be carried out to adapt the design to robotic TLM surgery along with addition of DOF in the device with introduction

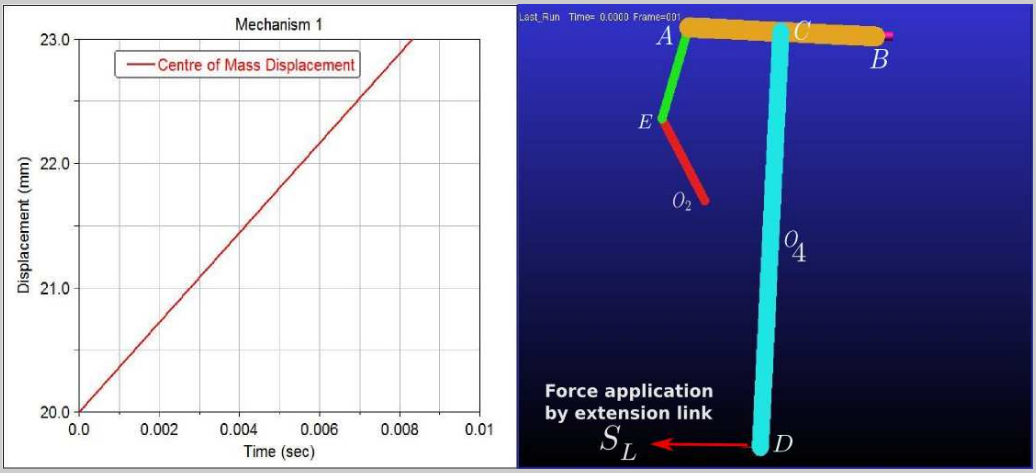

(a) Validation of Mechanism 1

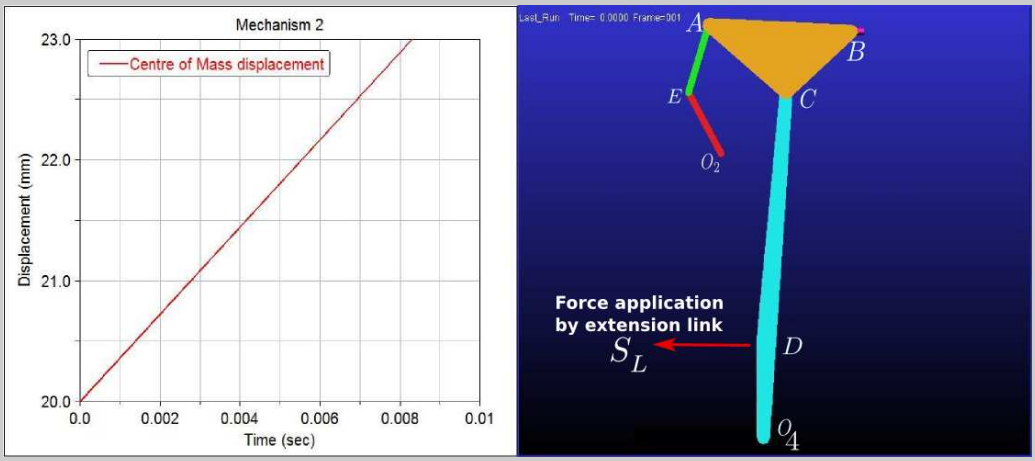

(b) Validation of mechanism 2

Figure 8. ADAMS Model Validation

of flexible modular tool shaft. This additional DOF will increase the reach of the microsurgical forceps within the TLM surgical procedures.

REFERENCES

[1] P. A. Liverneaux, S. H. Berner, M. S. Bednar, S. J. Parekattil, G. M. Ruggiero, and J. C. Selber, *Telemicrosurgery: robot assisted microsurgery*. Springer Science & Business Media, 2012.

[2] M. Remacle, G. Lawson, M.-C. Nollevaux, M. Delos *et al.*, "Current state of scanning micromanipulator applications with the carbon dioxide laser," *Annals of Otology, Rhinology & Laryngology*, vol. 117, no. 4, p. 239, 2008.

[3] B. Simpson and C. Rosen, "Principles of phonomicrosurgery," *Operative Techniques in Laryngology*, pp. 63–76, 2008.

[4] M. Hirano, "Morphological structure of the vocal cord as a vibrator and its variations," *Folia Phoniatrica et Logopaedica*, vol. 26, no. 2, pp. 89–94, 1974.

[5] S. Wang, Q. Li, J. Ding, and Z. Zhang, "Kinematic design for robot-assisted laryngeal surgery systems," in *Intelligent Robots and Systems, 2006 IEEE/RSJ International Conference on*. IEEE, 2006, pp. 2864–2869.

[6] Tuebingen Scientific's "art 2 DRIVE" for laparoscopic surgery. Accessed on 21-Feb-2016. [Online]. Available: http://www.tuebingen-scientific.com/Standard/produktnavigation/drive/zusammenfassung/

[7] Tuebingen Scientific's "art 2 CURVE" for single port surgery. Accessed on 21-Feb-2016. [Online]. Available: http://www.tuebingen-scientific.com/Standard/produktnavigation/curve/zusammenfassung/

[8] SILS^{TM} Hand Instruments. Accessed on 21-Feb-2016. [Online]. Available: http://www.medtronic.com/covidien/products/hand-instruments-ligation/sils-hand-instruments

[9] SerpENT Articulating Instruments. ENTrigue Surgical Inc. Accessed on 21-Feb-2016. [Online]. Available: http://www.ent-surg.com/home/US_products/serpent

[10] M. Van Veelen, D. Meijer, R. Goossens, and C. Snijders, "New ergonomic design criteria for handles of laparoscopic dissection forceps," *Journal of Laparoendoscopic & Advanced Surgical Techniques*, vol. 11, no. 1, pp. 17–26, 2001.

[11] J. Kaljun and B. Dolšak, "Ergonomic design knowledge built in the intelligent decision support system," *International Journal of Industrial Ergonomics*, vol. 42, no. 1, pp. 162–171, 2012.

[12] S. Pheasant and C. M. Haslegrave, *Bodyspace: Anthropometry, ergonomics and the design of work*. CRC Press, 2005.

[13] N. A. Stanton, M. S. Young, and C. Harvey, *Guide to methodology in ergonomics: Designing for human use*. CRC Press, 2014.

[14] G. Gogu, "Chebychev–grübler–kutzbach's criterion for mobility calculation of multi-loop mechanisms revisited via theory of linear transformations," *European Journal of Mechanics-A/Solids*, vol. 24, no. 3, pp. 427–441, 2005.